Physical modelling of forest fire spreading through heterogeneous fuel beds

Physical modelling of forest fire spreading through heterogeneous fuel beds

Suggested running head: Fire spread through heterogeneous fuels

Albert Simeoni [a,d] *Pierre Salinesi* [b] *and Frédéric Morandini* [c]

[a] Department of Fire Protection Engineering, Worcester Polytechnic Institute, Worcester, MA 01609, USA

[b] Fire Department of South-Corsica, BP 552, 20189 Ajaccio cedex 2, France

[c] UMR CNRS 6134 – SPE, University of Corsica, BP 52, 20250 Corte, France

[d] Corresponding author. Email: asimeoni@wpi.edu

Abstract

Vegetation cover is a heterogeneous medium composed of different kinds of fuels and non-combustible areas. Some properties of real-fires arise from this heterogeneity. Creating heterogeneous fuel areas may be useful both in land management and in fire fighting by reducing the fire intensity and the fire rate of spread. The spreading of a fire through a heterogeneous medium was studied by a two-dimensional reaction-diffusion physical model of fire spread. Randomly distributed combustible and non-combustible square elements constituted the heterogeneous fuel. Two main characteristics of the fire were directly computed by the model: the size of the zone influenced by the heat transferred from the fire front and the ignition condition of vegetation. The model was able to obtain rate of fire spread, temperature distribution and energy transfers. The influence on the fire properties of

the ratio between the amount of combustible elements to the total amount of elements has been studied. The results provided the same critical fire behaviour as described in both percolation theory and laboratory experiments but the results were quantitatively different because the neighbourhood computed by the model varied in time and space with the geometry of the fire front. The simulations also qualitatively reproduced fire behaviour for heterogeneous fuel layers as observed in field experiments. This study shows that physical models can be used to study fire spreading through heterogeneous fuels and some potential applications are proposed about the use of heterogeneity as a complementary tool for fuel management and fire-fighting.

Additional keywords: Fire critical behaviour, non-combustible zones, reaction-diffusion model, surface fire spread.

Introduction

The main physical forest fire spread models describe the fire spreading through homogeneous fuels (Pastor et al. 2003). However in the field, homogeneous fuel beds are extremely rare (Brown 1982); vegetation cover is a heterogeneous medium including different kinds of fuels and non-combustible areas (Bradstockl and Gill 1993). Some of the fires' properties can arise from this heterogeneity, for instance, the development of fire fingers (Caldarelli et al. 2001). Real-fires also display thresholds for spreading that depend on environmental factors such as wind and fuel moisture content (Cheney et al. 1993, Marsden-Smedley et al. 2001, Weise et al. 2005). The fire regimes are partly a consequence of a coupling between heterogeneous patterns of vegetation and past fires (Baker 1989, Miller and Urban 1999).

The work described in this paper is motivated by the necessity of developing new approaches in land management and in fire-fighting. The field experience of the first two

50 authors as fire-fighters has shown them that fire-fighting as well as fuelbreaks can become
51 ineffective during extreme events (strong winds, large-scale fires or steep canyons for
52 instance). Artificially controlling the fuel heterogeneity may be useful to reduce fire hazard
53 (Loehle 2004, Finney et al. 2007).

54 The critical behaviour of forest fires has been investigated in details thanks to the
55 percolation theory (Stauffer, 1985). This approach allows better understanding of the forest
56 fire behaviour at the field scale (Ohtsuki and Keyes 1986, Von Niessen and Blumen, 1986)
57 and the interactions between fires and forest growth (Drosswel and Schwabl, 1992, Malamud
58 et al. 1998). Other studies focused on the critical behaviour of fire spreading at the laboratory
59 scale (Beer and Enting 1990, Nahmias et al. 2000).

60 In percolation-type models, the assumptions used to propagate the fire are not
61 physically based (Weber 1990) and the critical thresholds are directly dependent on the
62 assumptions made to build the models; this has been recognised as quite naive (Beer and
63 Enting 1990). For instance, the probability of ignition of a tree or the definition of the
64 neighbourhood of a burning plot – that is to say the other pieces of vegetation influenced by
65 this burning plot – are constant in space and time. These quantities must be known *a priori*. In
66 a real fire they vary with time and position. They also depend strongly on the fire front
67 geometry and on vegetation as a fuel. This approach has permitted the modelling of the
68 critical behaviour of forest fires at the landscape scale, and they are used to study the long-
69 term interaction with forest growth and fire (Drossel and Schwabl 1992). The application of
70 percolation-type fire spread models to the study of single fires is more limited because they
71 do not provide the primary outputs, such as rate of fire spread or heat fluxes, which are
72 necessary for forest managers and fire-fighters. Furthermore these models are very difficult to
73 validate as, in real fires it is difficult to discriminate percolation effects from the influence of

74 the external conditions (wind, vegetation moisture content, topography and so on, see
75 Tephany and Nahmias 2002 and Weise et al. 2005).
76 A recent approach based on the Small World Network combines physical modelling
77 and percolation theory (Zekri et al. 2005). It provides very short calculation times but it
78 necessitates the implementation of some physical parameters, as combustion time, time of
79 degradation before ignition and long-range radiation effects. These parameters are obtained
80 from physical modelling but they do not vary with time, position and front shape.
81 More recently, empirical fire spread models were used to assess the influence of
82 heterogeneities made by prescribed burnings on the occurrence of unexpected fires (King et
83 al. 2008). The results showed the role of heterogeneous fuels in decreaseing fire size and
84 intensity; they highlighted the need for more studies of this kind.
85 A convenient way to simulate the fire spread through heterogeneous fuel layers is by
86 using Cellular Automata. They use a cellular mesh with each cell having a defined state (such
87 as burned and unburned), a neighborhood and rules for the change in cell state. The rules use
88 mathematical formulas to define the change in sate of the cells along time. The rules are based
89 on the fire spread mechanisms. To define the rules, some approaches use percolation (Duarte
90 et al. 1992) and others use semi-empirical models (Berjak and Hearne 2002). A detailed
91 analysis can be found in the reviews by Perry (1996) and Sullivan (2009).
92 The main objective of this paper is to evaluate the ability of physical modelling to
93 study the properties of wildland fire spreading through heterogeneous fuels. To proceed, a
94 two-dimensional reaction-diffusion model was used. The model includes a sub-model for
95 long-range radiative transfer and was validated at the laboratory scale for homogeneous fuel
96 beds (Morandini et al. 2005). The study focused on the properties of a single fire spread. The
97 non-homogeneous fuel consisted of combustible and non-combustible square elements
98 randomly distributed with a fixed ratio. Such a model (and physical models generally) directly

99 determines the neighbourhood thermally influenced by the fire front and the ignition of
100 vegetation from physical considerations. These quantities are dependent on many parameters,
101 such as vegetation species, moisture contents, wind, slope and so on. The model also provides
102 the fire rate of spread, the temperature distribution, as well as the energy transfers. In this
103 paper, the model simulations were qualitatively compared to experimental results and studies
104 conducted both at laboratory and field scales.

105 In the next sections, the reaction-diffusion model and the numerical implementation
106 are detailed. Results of simulations representing different kind of fuel heterogeneities are then
107 presented and discussed; the simulations are compared qualitatively with theory and
108 experiments. A short discussion is then conducted about the potential applications for fuel
109 management and fire fighting that arise from this study. Finally, the conclusions are drawn
110 and some scientific perspectives are proposed.

111

112 **Numerical modelling**

113 *The physical model*

114 The main characteristics of the model are summarized below. Further details are available in
115 the paper by Morandini et al. (2005).

116 The model has been developed to represent the fire spread through fuel beds (such as
117 pine needle beds) and it has been validated at laboratory scale in terms of rate of spread,
118 temperature, fire front shape and heat transfer. It takes into account the thermal transfers that
119 are involved in the field, including long-range radiation. Thus, this model can be considered
120 suitable for bench-scale modelling of the fire spread through heterogeneous fuels in the field.
121 The main equation is a thermal balance on a medium equivalent to the fuel bed:

122 $$\frac{\partial T}{\partial t} + k_v \vec{V}_g . \vec{\nabla} T = -k(T - T_a) + K\Delta T - Q\frac{\partial \sigma_k}{\partial t} + R \qquad (1)$$

123 with the following boundary and initial conditions:

$$\vec{n}.\vec{\nabla}T = 0 \quad \text{at the fuel-bed boundaries,} \tag{2}$$

$$T_0 = T_a \quad \text{for an unignited cell at time zero,} \tag{3}$$

$$T_0 = T_{ig} \quad \text{for an ignited cell at time zero.} \tag{4}$$

Load variation along time for a burning cell is represented by:

$$\sigma_k = \sigma_{k_0} e^{-\alpha(t-t_{ig})} \tag{5}$$

where T and T_a represent the equivalent medium temperature and the ambient temperature respectively. The ignition time t_{ig} is defined as the time when the cell temperature reaches the ignition temperature. k is the cooling convection coefficient, K is the equivalent diffusion coefficient, Q is the combustion enthalpy and α is the combustion time constant. The coefficients of Eq. 1 are reduced coefficients as they are divided by the thermal mass per unit area of the medium equivalent, m. The model parameters (k, K, Q and α) are determined from a measured time-temperature curve obtained for a linear spread under no slope and no wind conditions (Santoni et al. 1999). The advective coefficient k_v is estimated as a thermal mass ratio (Simeoni et al. 2003). σ_k and σ_{k_0} are the fuel load and the initial fuel load, respectively. The radiative and convective terms are described in greater detail below.

With regard to the radiation term R in Eq. (1), the flame is assumed as being a radiant surface with a given height and constant temperature T_{fl} and emissivity ε_{fl} (Morandini et al. 2001). The amount of energy impinging the top of the fuel layer was calculated from the Stefan-Boltzmann law. The rate at which radiant energy from flame front is absorbed by the fuel element dS_v is:

$$\phi_{fl-dS_v} = a_v \, \varepsilon_{fl} \, B T_{fl}^4 \, F \tag{6}$$

where B is the Stefan-Boltzmann constant and a_v is the fuel bed coefficient of absorption. The view factor F depends on the flame length and tilt angle as follows (cf. Fig. 1):

147 $$F = \int_{S_{fl}} \frac{\cos\varphi_{fl}\,\cos\varphi_k}{\pi r^2}\, dS_{fl}\, dS_k \qquad (7)$$

148 Thus we obtain:

149 $$R = 0 \qquad \text{for a burning cell,} \qquad (8)$$

150 $$R = \frac{\phi_{fl-dS_v}}{m\, dS_v} = R^*\, F \qquad \text{for an unburned cell located ahead of the fire front,} \qquad (9)$$

151 where *m* represents the thermal mass of the fuel per unit area.

152 To express the convective term present in Eq. (1), the following equations for the flow

153 through the fuel layer are set (Simeoni et al. 2003):

154 $$\frac{\partial V_{g,x}}{\partial x} + \frac{V_{g,x}}{\rho_g}\frac{\partial \rho_g}{\partial x} = -\frac{V_{g,z}(\delta)}{\delta} - \frac{1}{\rho_g\,\delta}\frac{\partial \sigma_k}{\partial t} \qquad \text{in the burning zone,} \qquad (10)$$

155 $$V_{g,z}(\delta) = \chi\sqrt{2\delta\left(\frac{T}{T_a}-1\right) g\,\cos\phi_{sl}} \qquad \text{in the burning zone,} \qquad (11)$$

156 $$\rho_g T = \rho_a T_a \qquad \text{in the gas phase,} \qquad (12)$$

157 were δ is the height of the fuel layer, ϕ_{sl} is the slope angle and χ is a drag forces coefficient

158 (Simeoni et al. 2003). The model presented in Eqs. (1-9) is two-dimensional along the ground

159 shape (*x* and *y* directions). In order to take into account the buoyancy effects in the mass

160 balance for the gas phase (Eq. 7), the vertical velocity of the gas at the top of the fuel layer

161 $V_{g,z}(\delta)$ has to be described (cf. Fig. 2). This is done from the momentum equation along the

162 vertical axis (Eq. 8). Gas density is defined by using the isobaric perfect gas law (Eq. 9). To

163 close the model, the hypothesis of the thermal equilibrium between the gas and solid phases in

164 the fuel layer was set and the gas density was directly obtained from the temperature provided

165 by Eq. (1).

166

167 *Numerical implementation*

168 Following the assumption of a quasi-static flow, the system of equations was implemented in
169 a simple manner. The characteristic time of the coupled system was assumed to be the one of
170 the energy equation (Simeoni et al. 2003). The 4^{th} order Runge-Kutta method is used to solve
171 the equation describing local wind conditions (Butcher 2008). For the thermal balance, a
172 finite difference method was used. An "upwind" difference scheme (finite differences in the
173 direction of flow) was used to take into consideration the extent of convective transfers in the
174 wind direction (Patankar 1980). The resulting system of linear algebraic equations was then
175 solved using the Jacobi iterative method (Sibony and Mardon 1988). The mesh size was of
176 0.01 *m* while the time step varied from 0.1 *s* to 0.01 *s* in order to meet the Courant–
177 Friedrichs–Lewy (CFL) condition (Courant et al. 1928).
178 Table 1 shows the value of the model coefficients. They were established for a
179 homogeneous layer of 0.5 kg/m^2 *Pinus Pinaster* needles with 10 % moisture content
180 (Morandini et al. 2005). The model parameters h, K, Q and γ are determined from a measured
181 time-temperature curve obtained for a linear spread under no slope and no wind conditions
182 following the method proposed in Balbi et al. (1999). They are identified once for a given
183 fuel, fuel moisture content and fuel load and remain valid for all the experiments considered
184 hereafter, whatever the slope and wind. The flame length was set to 20 *cm* that represented the
185 mean experimental height of flame (Morandini et al. 2005). The diffusion coefficient K was
186 decreased by 40 % in comparison with Morandini et al. (2005). Indeed, the energy equation
187 (1) was solved over the whole domain and diffusion losses between fuel cells (at a
188 temperature greater than the ambient temperature) and empty cells (remaining at the ambient
189 temperature) were over-estimated. The K coefficient represents a global diffusion of heat that
190 includes the basic contribution of radiation from the bottom of the flame and from the embers
191 inside the fuel layer (Balbi et al. 1999). To take into account this part of the radiative transfer
192 and to better account for the long-range radiative transfer from the flame, which is enhanced

193 for heterogeneous fuels, the radiative coefficient R^* was increased by 20 % in comparison
194 with Morandini et al. (2005).

195 The spreading domain was composed of a homogenous area at the left hand side
196 followed by a heterogeneous zone. The non-homogeneous fuel consisted of combustible and
197 non-combustible square elements randomly distributed with a fixed ratio. The fuel
198 distribution was created with a random number generator. A number between 0 and 1 was
199 attributed to each cell of the domain. Then, each cell with a number lower than the fixed
200 fraction of combustible elements (for instance 0.6 for 60 % of fuel and 40 % of empty space
201 in the domain) was filled with fuel and each cell with a number higher than the ratio was left
202 empty. The neighbourhood influenced by the fire front and the ignition of vegetation were
203 directly computed by the model. Each vegetation element was made with a square of four
204 mesh cells. This arbitrary choice was made to allow for both long-range effects of radiation
205 and the critical behaviour of the fire. The tests were performed to assess the model ability to
206 represent real fire behaviour and to consider different possibilities of using fuel heterogeneity
207 both in land management and in fire-fighting.

208 A straight line ignition was initiated at the left hand side of the domain and the length
209 of the homogeneous zone was set in order to allow a fully developed fire reaching the
210 heterogeneous area. For each condition, the size of the domain was tested to avoid size effects
211 and at least 50 repetitions were completed to obtain mean values of the fire spread properties.

212 Several numerical test series were conducted under different conditions: slope vs. no
213 slope and wetted vs. dry fuels. As a first approach of the problem, wind configurations were
214 not studied as slope and wind effects were similar for forest fuel beds up to a threshold value
215 (Morandini et al. 2002).

216

217 **Results and discussion**

The simulations presented in the following section were performed to assess the model's ability to represent fire spreading through heterogeneous fuel layers and to discuss the relevance of developing heterogeneous fuel zones for fire fighting and prevention. The different cases studied hereafter include a vegetation pattern made with a mix of Combustible and Non Combustible areas for flat and upslope conditions, a fuel layer made heterogeneous by a mix of dry and wet areas for flat conditions and a combination of the two conditions (Non Combustible areas and wet fuels).

Flat conditions

The first test series was conducted under no slope conditions to evaluate the critical threshold for the fire spread and the effects of heterogeneity on the rate of fire spread. The critical threshold is defined as the status between fire spread success and fire spread stop.

Figure 3 shows the effect of the fraction of combustible elements (FCE) on the rate of fire spread. The threshold was found to be equal to 0.5. It can be seen that near the critical value, the fire rate of spread is almost half the one for the homogeneous fuel (FCE = 1). The rate of spread decreases slowly to the FCE value of 0.52. Then, it decreases steeply to the threshold value of 0.5. This critical behaviour has been observed both in laboratory experiments (Téphany et al. 1997, Nahmias et al. 2000) and in the field (Bradstockl and Gill 1993, Cheney et al. 1993).

The threshold value is lower than the theoretical one found in percolation theory with a Von-Neumann neighbourhood (0.593 for 4 elements with an adjacent side to the considered one) but higher than the theoretical one with a Moore neighbourhood (0.407 for the 8 adjacent elements) (Stauffer 1985). This result implies that the mean neighbourhood for the whole fire front has a configuration between the two previous ones. In the simulations and in real fires,

242 the neighbourhood of a burning element changes with time as it depends on the radiation
243 transferred ahead of the fire front.

244 To further study the role heterogeneous fuel beds in fire prevention, an area was
245 simulated with two heterogeneous zones (FCE of 0.55 and 0.51). This configuration was
246 chosen because it corresponds to a possible cleaning at the boundaries of a fuelbreak. Figure 4
247 shows a fire spreading in such a configuration. The addition of two zones with FCE over the
248 threshold value (0.5) did not stop the fire as expected but it decreased the rate of spread by
249 35 % in the first zone and by 46 % in the second zone (see table 1). With the heterogeneous
250 domain, the propagation time was increased by around 60 % in comparison with the
251 homogeneous domain. Another interesting effect, shown by Fig. 4 was the decrease in width
252 of the fire front. This effect was systematically observed for all repetitions of the simulations
253 (around 50) and it causes a lower amount of radiation to be sent ahead of the fire front.

254 The effect of the number of burned elements on distance and time was also studied.
255 Percolation theory (Stauffer 1985) and experiments (Beer and Enting 1990, Téphany et al.
256 1997, Namias et al. 2000) show a power-law dependence for this quantity. A similar
257 dependence was obtained with the model but the coefficients were greater than the theoretical
258 ones. This was due to the difference in conditions between the simulations conducted in this
259 work and the percolation studies that consider simple neighbourhoods. Indeed, Téphany et al.
260 (1997) and Nahmias et al. (2000) designed their experiments to match the theoretical
261 neighbouroods; in contrast, the model coefficients were in the same range as those obtained
262 for fire spread under more realistic experimental conditions (Beer and Engins 1990). As there
263 is little data available in literature, this aspect should be further investigated in the form of
264 experiments dedicated to the critical behaviour of forest fires. This objective is clearly beyond
265 the scope of the present paper that is devoted to the evaluation of the relevance of physical
266 modelling to study heterogeneous fuel layers in the context of fire prevention.

Slope conditions

The influence of slope was also analyzed. Figure 5 displays the burned elements at the end of the spreading for a 0.31 FCE and a 10° slope. The upslope direction is shown by an arrow. For this slope, 0.31 FCE was found to be the threshold value. As was seen previously for flat conditions, a slight change in the FCE value (from 0.31 to 0.32) induced a change in the fire regime and demonstrated that the model is able to describe the critical fire behaviour. This value is lower than 0.5 for flat conditions because of the increased heat transfers in the slope direction. Fire fingers developed, as observed in experiments at laboratory scale (Téphany et al. 1997). This behaviour has also been observed for wildfires in heterogeneous areas (Caldarelli et al. 2001), though it must be acknowledge that fire fingers can also be caused by other parameters (changing in wind, uneven ground, infrastructure etc.). The main finger did not reach to the edge of the domain because its width reduced with time (as an effect of the random distribution of empty elements and as the FCE was equal to the critical value).

Figure 5 also shows the long-range ignition of combustible elements. In the main spreading direction, the fire front ignited combustible cells even if empty cells were located in between them. This was mainly due to the radiative contribution of the tilted flames in the slope direction as computed by the model. At the sides of the finger, adjacent cells did not burn because the heat transfers were lower. This long-range ignition has been observed in laboratory experiments with square elements of wood shavings (Téphany et al. 1997). The authors have also observed it in wildfires but it must be validated by field experiments as the potential causes (radiation or firebrands) are very difficult to separate during uncontrolled fires.

It should be noted that sometimes the combustible cells located at the border of non-combustible zones did not burn (see Figs. 4 and 5) as they were cooled by diffusion losses with the adjacent empty cells. This effect remains to be validated in the field as it is generally

observed that continuous pieces of vegetation (with low moisture contents) often burn entirely.

Figure 6 shows the temperature distribution at the intermediate time t = 50 s for the same test as depicted in Fig. 5. One can note the end of the spread through the homogeneous zone at the boundaries of the domain (where high temperatures were present). This figure illustrates the long-range radiant effect of the model. The neighbourhood (that is to say the cells that are heated up by the fire front) of the large fire finger in the middle of the domain is very different from the ones of the narrow fingers at the upper and lower parts of the domain. The fuel cells located in front of the large finger are heated 20 cm ahead of the fire front whereas the cells located in front of the small fingers are only heated up to 8 cm. The short-range effect for narrow fingers and the long-range effect for large fingers are due to the neighbourhood calculated by the model that varies with the *fire* front shape. This property is not represented by other models based on percolation theory that consider a constant neighborhood for the burning cells, whatever the fire front shape (Ohtsuki and Keyes 1986, Von Niessen and Blumen 1986, Drossel and Schwabl 1992, Zekri et al. 2005). The fire fingers observed in Figs. 5 and 6 correspond to the same effect leading to a narrow fire front in Fig. 4.

Wetted heterogeneous zones

The last type of fuel heterogeneity considered in this work was that of water. The domain was constituted by a homogeneous fuel with randomly wetted elements. These conditions simulated the random water supply on a fuel bed by spraying. The additional water was assumed to remain outside vegetation. If one considers a fuel cell, the external water acts as a sink source prior to ignition. Thus, a sink term due to the vaporization of vapour at $100°C$ is added to Eq. (9) until all the mass of external water has evaporated. Moisture content

317 represents the amount of water inside vegetation and it is indirectly included in the model
318 coefficients h, K, Q and γ (Balbi et al. 1999). Several tests were conducted and an example is
319 depicted in Fig. 7. It represents the arrival of a fire front on a heterogeneous wetted zone with
320 a fraction of wetted elements (FWE) of 0.6. Each of these contained 70 % water, added on the
321 basis of the fuel load (almost dry fuel). When it reached the heterogeneous zone, the fire front
322 dried the cells located just in front of it; for example, the white zone circled in Fig. 7 as an
323 example). Nevertheless, the FWE value was high and it did not allow the fire to propagate.
324 Further simulations were conducted for a lower FWE value (0.5). Even if the fire
325 spread over the whole domain, the decrease in the rate of spread was substantial compared to
326 a homogeneous dry medium (having a 10 % residual moisture content); it spread at half the
327 rate. Furthermore, some unburned areas remained, corresponding to big clusters of wetted
328 elements, as shown in Fig. 8. This phenomenon was observed both in laboratory and field
329 experiments for fuel elements wetted by sprinklers (Nahmias et al. 2000) and for particularly
330 wet vegetation (Santoni et al. 2006).
331 The configuration used for the simulations is similar in nature as the configuration
332 used by Finney (2003) for fuel mixed with very slow-burning fires. However, neither fire-
333 finger nor unburned patched were observed because all fuels burned totally.
334 The last test evaluated the influence of the moisture content on the threshold value.
335 Heterogeneous areas were considered with wetted vegetation elements and empty elements. A
336 non-spreading configuration was reached with 40 % of water and a 0.4 FCE. As expected, the
337 necessary FCE value that prevented the fire from spreading was low (see the field experiment
338 conducted by Nahmias et al. 2000). Merging the two processes allowed the FCE to be
339 increased substantially to reach the no-spread threshold and it decreased further the spreading
340 time with respect to the dry configuration.
341

342 *About some potential applications*

343 Some potential applications of heterogeneous fuels are described in this section and complete
344 the thoughts preented in Nahmias et al. (2000). These potential applications are only the two
345 first authors' perspectives and are a consequence of their joint work in the field and in the
346 laboratory. Obviously, they need to be scientifically studied before any implementation in the
347 field.

348 Considering land management, the efficiency of fuelbreaks could be increased by
349 heterogeneous areas located on their two sides. This would decrease both the rate of spread of
350 a fire reaching a fuelbreak and the fire front width (as displayed in Fig. 4). The heterogeneous
351 strip on the other side of the fire front arrival would also decrease the probability of ignition
352 by firebrands.

353 The Wildland-Urban Interface could be treated as heterogeneous buffer zones. The
354 heterogeneity effect could even be increased by using the distribution of Non Combustible
355 Areas in urban development planning such as houses, car parks, roads and so on (Spyratos et
356 al. 2007). A fire reaching these heterogeneous zones would break in several fingers and
357 produce the same benefits as described in this paper for fuel breaks.

358 Concerning fire-fighting, the technique of putting as much water as possible on the
359 fire front to stop it becomes ineffective under extreme conditions. Figures 7 and 8 show that
360 the fire dynamics is reduced by heterogeneous zones created by randomly wetting the fuel.
361 Heterogeneous areas randomly pre-seeded with water or fire retardant before the arrival of the
362 fire front could create safer conditions for ground fighting and increase wildland/urban
363 interface protection. Sprinklers randomly distributed in the borders of the wildland/urban
364 interface could improve passive fire protection while saving water.

365 Finally, the combination of random fuel suppression and random wetting before the
366 fire arrival (corresponding to the last case discussed in the previous section) could be used to

367 combine several heterogeneity effects in order to decrease vegetation removal and the
368 associated costs in heterogeneous areas while maintaining a significant effect on the fire.
369
370 **Conclusions**
371 Different configurations of heterogeneous vegetation have been tested with a physical model.
372 The influence of the heterogeneity of vegetation on the critical behaviour of the fire spread
373 has been studied. The value of the fire spread rate and the evolution of the fire shape have
374 also been examined.
375 The simulations showed the relevance of using physical modeling to describe fire
376 behaviour in heterogeneous fuels. The model allowed to represent qualitatively the fire
377 behaviour for laboratory and field experiments. Physical models represent an efficient tool to
378 study these problems as they provide many outputs that can be useful for fire-fighting and fire
379 management such as fire shape, rate of fire spread and time for a fire to cross a heterogeneous
380 zone.
381 A short discussion has been conducted about the potential application of using
382 heterogeneous fuels in forest and Wildland-Urban Interface management and protection.
383 Table 2 presents an overview of the results obtained for the different configurations
384 used in this study. It was concluded that combining the different processes creating
385 heterogeneity improves the efficiency of heterogeneous zones.
386 Nevertheless, as there are only few experiments available in literature for
387 heterogeneous fuels, both laboratory and field experiments have to be conducted to test and
388 validate quantitatively the simulation results of physical models.
389
390
391

392 **References**

393 Balbi JH, Santoni PA, DupuyJL (2000) Dynamic modelling of fire spread across a fuel bed.
394 *International Journal of Wildland Fire*, **9**(4), 275-284.

395 Baker T (1989) Effect of scale and spatial heterogeneity on fire-interval distributions.
396 *Canadian Journal of Forest Research* **19**, 700-706.

397 Beer T, Enting IG (1990) Fire spread and percolation modelling. *Mathematical and computer*
398 *modelling* **13**(11), 77-96.

399 Berjak SG, Hearne JW (2002) An improved cellular automaton model for simulating fire in a
400 spatially heterogeneous Savanna system. *Ecological Modelling* **148**(2), 133-151.

401 Bradstock RA, Gill AM (1993) Fire in semi-arid, mallee shrublands: size of flames from
402 discrete fuel arrays and their role in the spread of fire. *International Journal of Wildland*
403 *Fire* **3**, 3-12.

404 Brown KB (1982) Fuel and Fire Behavior Prediction in Big Sagebrush. USDA Forest Service,
405 Intermountain Forest and Range Experiment Station Research Paper INT-290. (Ogden,
406 UT)

407 Butcher J (2008) Numerical Methods for Ordinary Differential Equations, 2nd Ed. John Wiley
408 & Sons, Hoboken, NJ.

409 Caldarelli G, Frondoni R, Gabrielli A, Montuori M, Retzlaff R, Ricotta C (2001) Percolation
410 in real wildfire. *Europhysics Letters* **56**, 510-518.

411 Cheney NP, Gould JS, Catchpole WR (1993) The influence of fuel, weather and fire shape
412 variables on fire-spread in grasslands. *International Journal of Wildland Fire* **3**, 31-44.

413 Courant R, Friedrichs K, Lewy H (1928) Über die partiellen Differenzengleichungen der
414 mathematischen Physik. *Mathematische Annalen*, **100**(1), 32-74.

415 Drossel B, Schwabl F (1992) Self-organized critical forest-fire model. *Physical Review*
416 *Letters* **69**, 1629-1632.

417 Duarte JAMS, Carvalho JM, Ruskin HJ (1992) The direction of maximum spread in
418 anisotropic forest fires and its critical properties. *Physica A: Statistical and Theoretical*
419 *Physics* **183**(4), 411-421.
420 Finney MA (2003) Calculation of fire spread rates across random landscapes. *International*
421 *Journal of Wildland Fire* **12**(2), 167-174.
422 Finney MA, Seli RC, McHugh CW, Ager AA, Bahro B, Agee JK (2007) Simulation of long-
423 term landscape-level fuel treatment effects on large wildfires. *International Journal of*
424 *Wildland Fire* **16**, 712-727.
425 King KJ, Bradstock RA, Cary GJ, Chapman J, Marsden-Smedley JB (2008) The relative
426 importance of fine-scale fuel mosaics on reducing fire risk in south-west Tasmania,
427 Australia. *International Journal of Wildland Fire* **17**, 421-430.
428 Loehle C (2004) Applying landscape principles to fire hazard reduction. *Forest Ecology and*
429 *Management* **198**, 261-267.
430 Malamud BD, Morein G, Turcotte DL (1998) Forest Fires: An Example of Self-Organized
431 Critical Behavior. *Science* **281**, 1840-1842.
432 Marsden-Smedley JB, Catchpole WR, Pyrke A (2001) Fire modelling in Tasmanian
433 buttongrass moorlands. IV. Sustaining versus non-sustaining fires. *International Journal*
434 *of Wildland Fire* **10**, 255-262.
435 Miller C, Urban DL (1999) Interactions between forest heterogeneity and fire regimes in the
436 Southern Sierra Nevada. *Canadian Journal of Forest Research* **29**, 202-212.
437 Morandini F, Santoni PA, Balbi JH (2001) The contribution of radiant heat transfer to
438 laboratory-scale fire spread under the influences of wind and slope. *Fire Safety Journal*
439 **36**(6), 519-543.

440 Morandini F, Santoni PA, Balbi JH, Ventura JM, Mendes-Lopes JM (2002) A two-
441 dimensional model of fire spread across a fuel bed including wind combined with slope
442 conditions. *International Journal of Wildland Fire* **11**, 53–64.
443 Morandini F, Simeoni A, Santoni PA, Balbi JH (2005) A model for the spread of fire across a
444 fuel bed incorporating the effects of wind and slope. *Combustion Science and*
445 *Technology* **177**, 1381-1418.
446 Nahmias J, Téphany H, Duarte J, Letaconnoux S (2000) Fire spreading experiments on
447 heterogeneous fuel beds. Applications of percolation theory. *Canadian Journal of*
448 *Forest Research* **30**, 1318-1328.
449 Ohtsuki T, Keyes T (1986) Biased percolation forest fires with wind. *Journal of Physics A* **19**,
450 281-287.
451 Pastor E, Zarate L, Planas E, Arnaldos J (2003) Mathematical models and calculation systems
452 for the study of wildland fire behaviour. *Progress in Energy and Combustion Science*
453 **29**, 139-153.
454 Patankar SV (1980) Numerical Heat Transfer and Fluid Flow. *Hemisphere Publishing*
455 *Corporation*, 198 p.
456 Perry GLW (1998) Current approaches to modelling the spread of wildland fire: a review.
457 *Progress in Physical Geography* **22**(2), 222-245.
458 Santoni PA, Balbi JH, Dupuy JL (1999) Dynamic modelling of upslope fire growth
459 *International Journal of Wildland Fire* **9**(4), 285-292.
460 Santoni PA, Simeoni A, Rossi JL, Bosseur F, Morandini F, Silvani X, Balbi JH, Cancelieri D,
461 Rossi L (2006) Instrumentation of wildland fire: characterisation of a fire spreading
462 through a Mediterranean shrub. *Fire Safety Journal* **41**, 171-184.
463 Sibony M, Mardon JC (1988) Approximations et équations différentielles. Hermann Eds.,
464 Paris.

Simeoni A, Santoni PA, Larini M, Balbi JH (2003) Reduction of a multiphase formulation to include a simplified flow in a semi-physical model of fire spread across a fuel bed. *International Journal of Thermal Science* **42**, 95-105.

Spyratos V, Bourgeon PS, Ghil M (2007) Development at the wildland-urban interface and the mitigation of forest-fire risk. *Proceedings of the National Academy of Sciences of the United States of America* **104**, 14272-14276.

Stauffer D (1985) 'Introduction to percolation theory.' (Taylor and Francis, London)

Sullivan AL (2009) Wildland surface fire spread modelling, 1990–2007. 3: Simulation and mathematical analogue models. *International Journal of Wildland Fire* **18**(4), 387-403.

Téphany H, Nahmias J, Duarte JAMS (1997) Combustion on heterogeneous media. A critical phenomenon. *Physica A* **242**, 57-69.

Téphany H, Nahmias J (2002) Comment on "Percolation in real wildfires" by G. Caldarelli et al. *Europhysic Letters* **59**, 155-156.

Von Niessen W, Blumen A (1986) Dynamics of forest fires as a directed percolation model. *Journal of Physics A* **19**, 289-293.

Weber RO (1990) A model for fire propagation in arrays. *Mathematical and computer modelling* **13**(12), 95-102.

Weise DR, Zhou X, Sun L, Mahalingam S (2005) Fire spread in chaparral – 'go or no go?'. *International Journal of Wildland Fire* **14**, 99-106.

Zekri N, Porterie B, Clerc JP, Loraud JC (2005) Propagation in a two-dimensional weighted local small-world network. *Physical Review E* **71**, 046121.

Table 1. Model parameters for a bed of *Pinus pinaster* needles (fuel load of $0.5\ kg\ m^{-2}$ and moisture content of *10 %*)

model parameter	h (s^{-1})	K $(m^2\ s^{-1})$	Q $(m^2\ K\ kg^{-1})$	γ (s^{-1})	R^* $(K^{-3}\ s^{-1})$
value	41×10^{-3}	0.9×10^{-6}	2.34×10^{3}	0.35	2×10^{-4}

492 Table 2. Overview of the different simulated tests

493

Slope	*0°*	*0°*	*0°*	*10°*	*10°*	*0°*
FCE	*0.5*	*0.55 – 0.51*	*0.31*	*1*	*1*	*0.4*
Wetted elements	*No*	*No*	*No*	*70 %*	*70 %*	*40 %*
FWE	*0*	*0*	*0*	*0.6*	*0.5*	*1*
Spreading	*No*	*Yes*	*No*	*No*	*Yes*	*No*

494

495

496

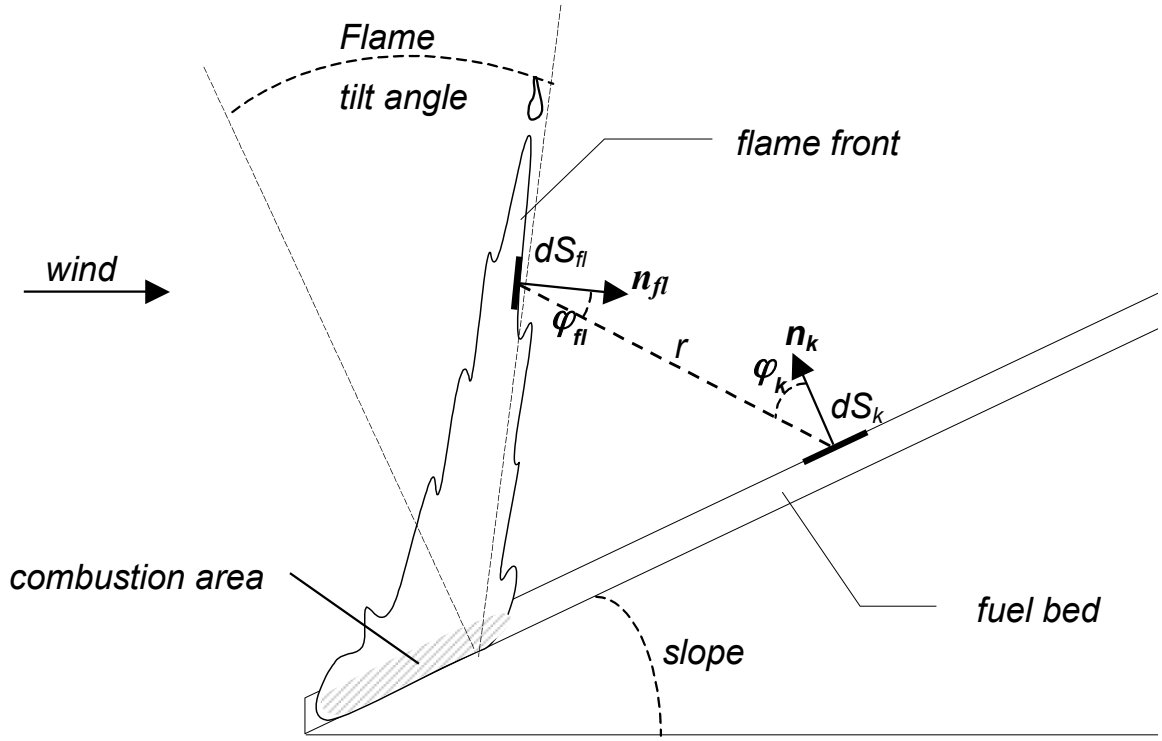

497

498 **Fig. 1.** Radiative transfers between two elementary surfaces of flame and fuel.

499

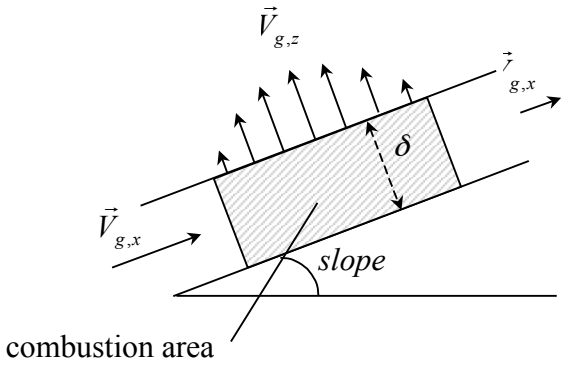

500

501 **Fig. 2.** Schematic representation of the flow within the fuel layer.

502

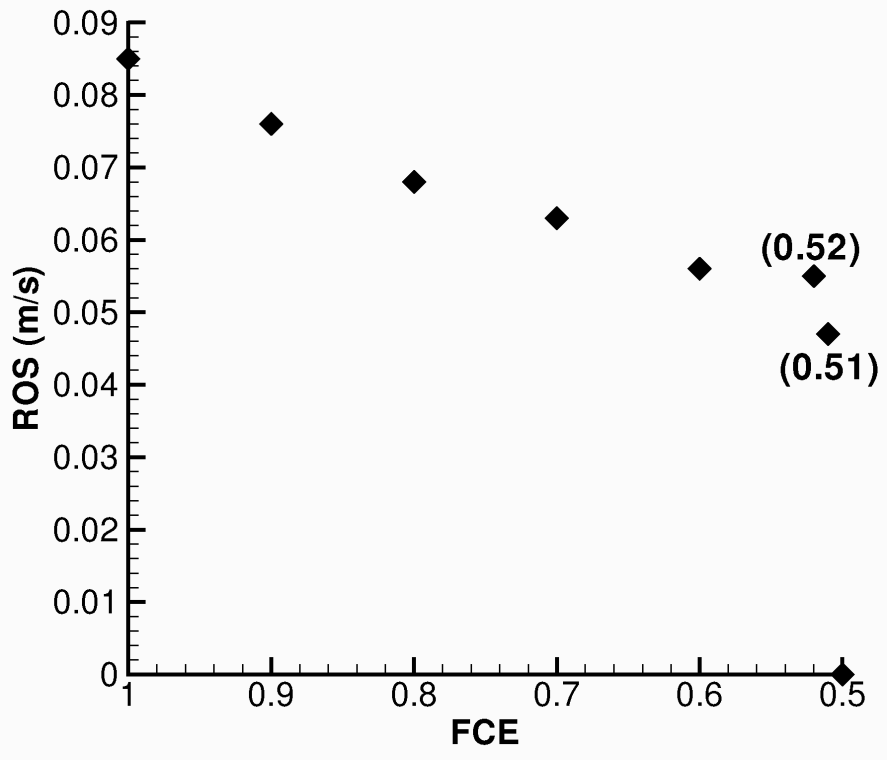

503

504

505 **Fig. 3.** Rate of fire spread as a function of the FCE for no slope

506

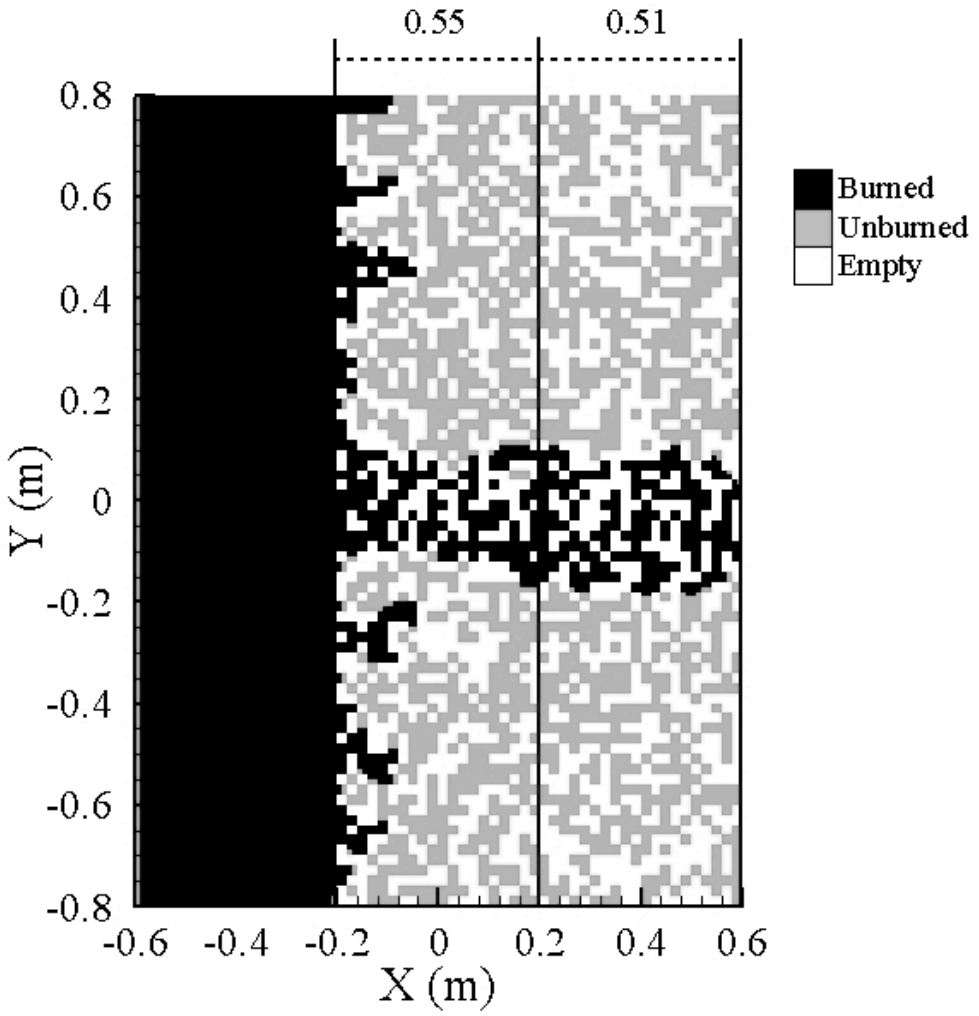

507

508

509 **Fig. 4.** Burned elements at the end of the spreading for a domain divided in 3 zones:

510 homogeneous, FCE = 0.55 and FCE = 0.51.

511

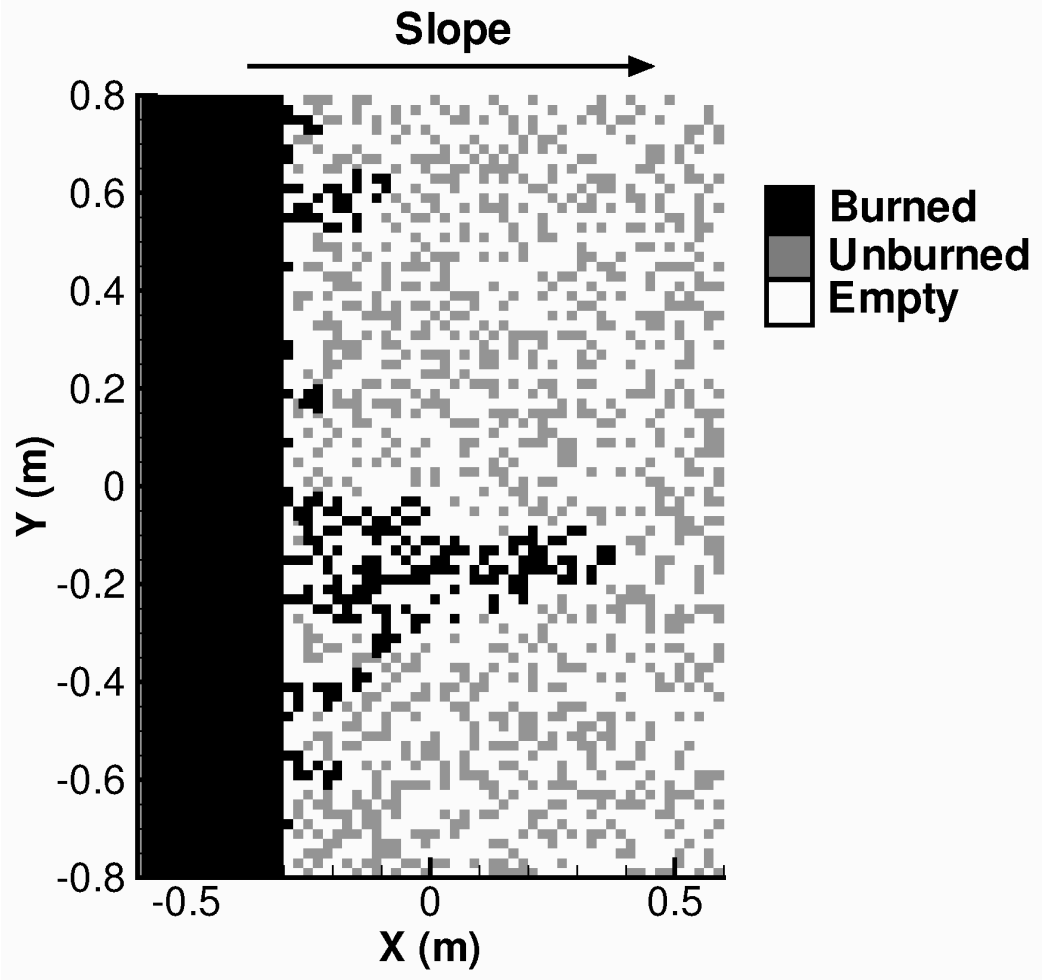

512

513

514 **Fig. 5.** Burned elements at the end of the spreading for a 0.31 FCE and a 10° slope.

515

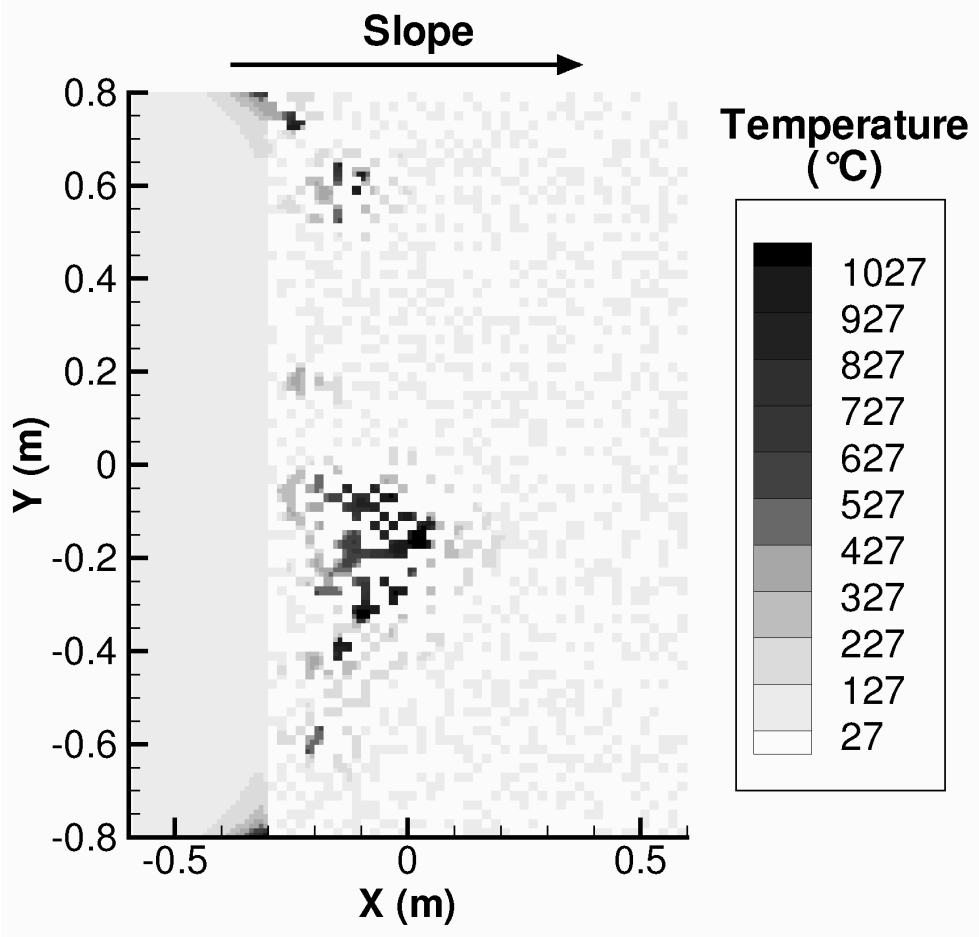

516

517

518 **Fig. 6.** Temperature distribution during the fire spread (t = 50 s) for a 0.31 FCE and a 10°

519 slope.

520

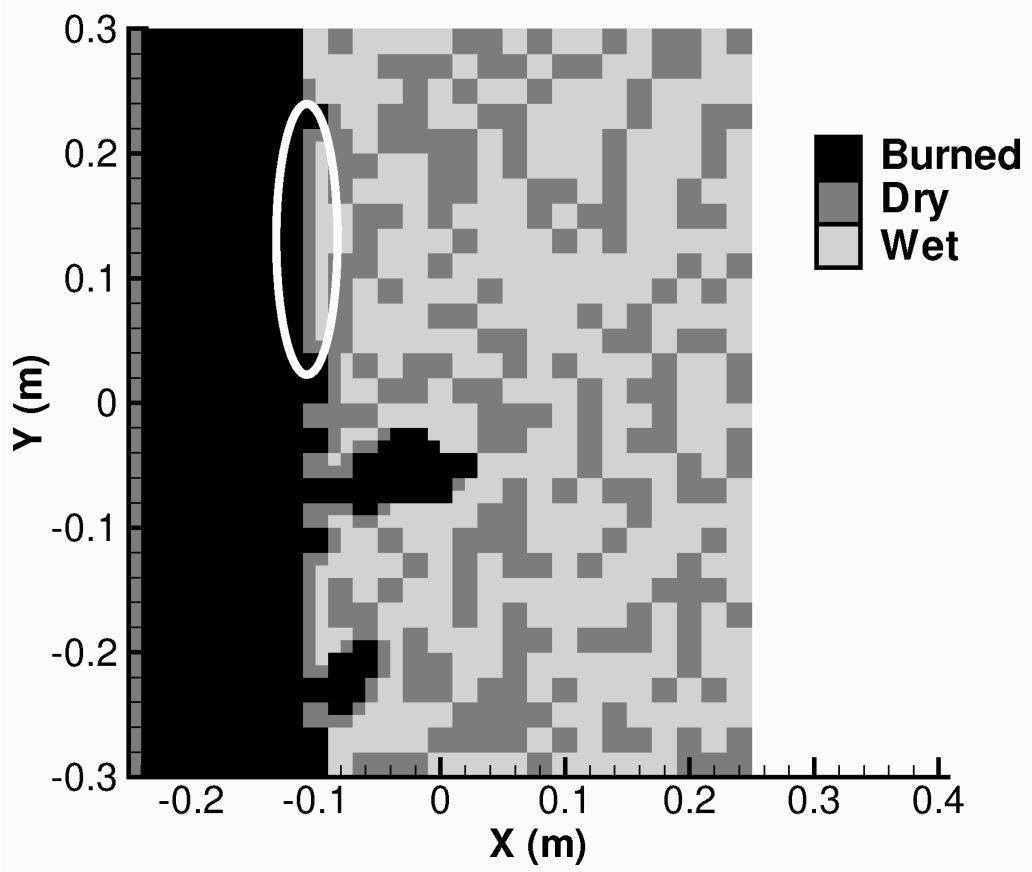

521

522

523 **Fig. 7.** Burned elements at the end of the spreading for a 0.6 FWE with 70 % of water and

524 no slope

525

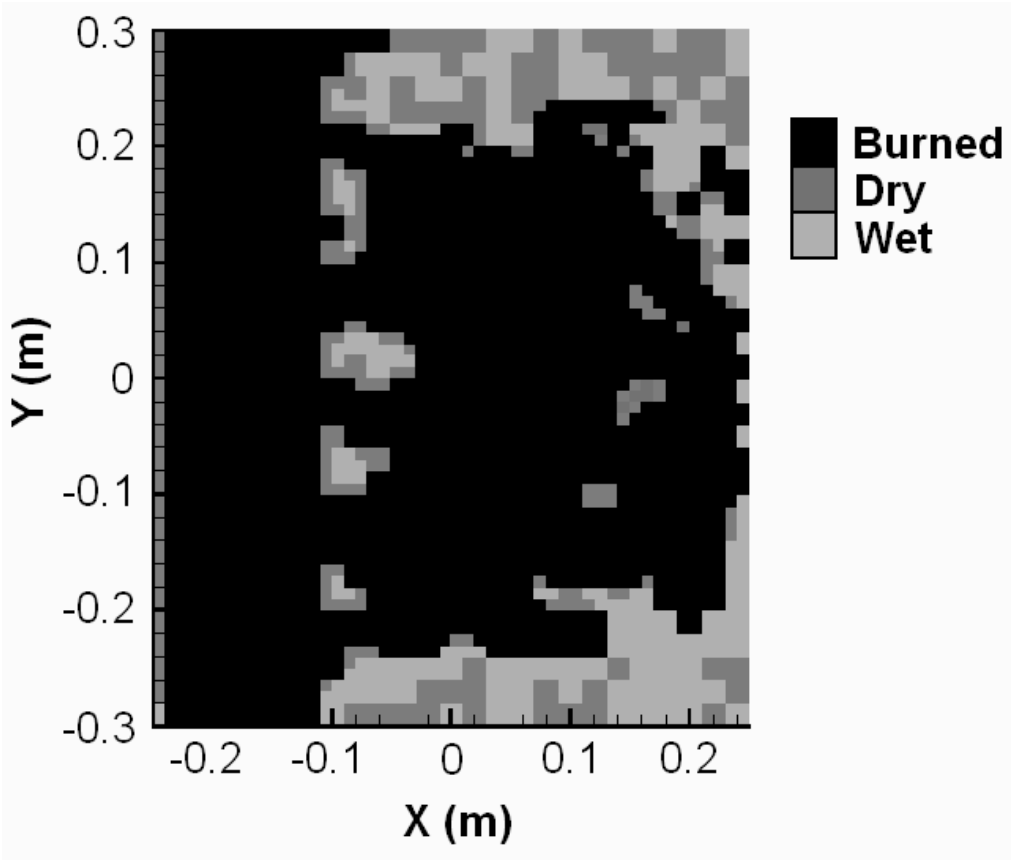

526

527

528 **Fig. 8.** Burned elements at the end of the spreading for a 0.5 FWE with 70 % of water and

529 no slope.